Targeted Elimination of Prostate Cancer by Genetically Directed Human T Lymphocytes

Terence P.F. Gade,[1] Waleed Hassen,[2] Elmer Santos,[3] Gertrude Gunset,[4,6] Aurore Saudemont,[6] Michael C. Gong,[2] Renier Brentjens,[4] Xiao-Song Zhong,[6] Matthias Stephan,[6] Jolanta Stefanski,[5] Clay Lyddane,[6] Joseph R. Osborne,[3] Ian M. Buchanan,[1] Simon J. Hall,[7] Warren D. Heston,[8] Isabelle Rivière,[4,5,6] Steven M. Larson,[3] Jason A. Koutcher,[1,3,4] and Michel Sadelain[4,5,6]

Departments of [1]Medical Physics, [2]Urology, [3]Radiology, and [4]Medicine; [5]Gene Transfer and Somatic Cell Engineering Facility, Memorial Sloan-Kettering Cancer Center; [6]Immunology Program, Sloan-Kettering Institute; [7]Department of Urology, Mount Sinai Medical Center, New York, New York; and [8]Department of Cancer Biology, Lerner Research Institute, Cleveland, Ohio

Abstract

The genetic transfer of antigen receptors is a powerful approach to rapidly generate tumor-specific T lymphocytes. Unlike the physiologic T-cell receptor, chimeric antigen receptors (CARs) encompass immunoglobulin variable regions or receptor ligands as their antigen recognition moiety, thus permitting T cells to recognize tumor antigens in the absence of human leukocyte antigen expression. CARs encompassing the CD3ζ chain as their activating domain induce T-cell proliferation *in vitro*, but limited survival. The requirements for genetically targeted T cells to function *in vivo* are less well understood. We have, therefore, established animal models to assess the therapeutic efficacy of human peripheral blood T lymphocytes targeted to prostate-specific membrane antigen (PSMA), an antigen expressed in prostate cancer cells and the neovasculature of various solid tumors. *In vivo* specificity and antitumor activity were assessed in mice bearing established prostate adenocarcinomas, using serum prostate-secreted antigen, magnetic resonance, computed tomography, and bioluminescence imaging to investigate the response to therapy. In three tumor models, orthotopic, s.c., and pulmonary, we show that PSMA-targeted T cells effectively eliminate prostate cancer. Tumor eradication was directly proportional to the *in vivo* effector-to-tumor cell ratio. Serial imaging further reveals that the T cells must survive for at least 1 week to induce durable remissions. The eradication of xenogeneic tumors in a murine environment shows that the adoptively transferred T cells do not absolutely require *in vivo* costimulation to function. These results thus provide a strong rationale for undertaking phase I clinical studies to assess PSMA-targeted T cells in patients with metastatic prostate cancer. (Cancer Res 2005; 65(19): 9080-8)

Introduction

Prostate cancer is the most frequent cancer in males in the United States and the cause of nearly 31,000 deaths per year (1). When diagnosed early, local adenocarcinomas can be effectively treated by radical extirpation or radiation (2, 3). Postsurgical residual disease requires radiation and/or hormonal therapy, which may prevent tumor progression and metastasis, but there is at present no curative treatment for hormone refractory, metastatic prostate cancer (4). Immunotherapy is a targeted therapy that is in principle an ideal approach for the treatment of minimal residual disease and micrometastases. The induction of cellular immunity requires that tumor antigens be presented in an immunogenic context, a far greater challenge for tumor antigens than for foreign molecules, such as viral antigens (5, 6). Successful immunization using dendritic cells or plasmid DNA vaccines (7–9) requires the presentation of human leukocyte antigen (HLA) class I–restricted peptides by both the antigen-presenting cell and the tumor itself. Immunogenic epitopes have been identified, at least for some HLA alleles, in antigens found in normal and transformed prostate cells, which include acid phosphatases, prostate-secreted antigen (PSA), prostate-specific membrane antigen (PSMA), and prostate stem cell antigen (10–13). Nonetheless, several obstacles remain to induce tumor immunity, which requires the expansion of cytotoxic T lymphocytes to numbers sufficient to mediate tumor rejection. Furthermore, the potency of the T-cell response may be undermined by several tumor escape mechanisms, which include antigen loss and HLA down-regulation, both of which deprive the T-cell receptor of its specific ligand on the surface of tumor cells (14).

The genetic engineering of T cells is a novel strategy designed to accelerate the generation of tumor-specific T cells and remedy the biological limitations that constrain the antitumoral functions of normal T cells. Chimeric antigen receptors (CARs) are essential constituents of this new armamentarium (15–18). Unlike the physiologic T-cell receptor, CARs encompass immunoglobulin variable regions or receptor ligands as antigen-recognition elements, thus permitting T cells to recognize cell surface tumor antigens in the absence of HLA expression (15–18). T-cell activation is mediated by the cytoplasmic domain of the CAR, which is typically derived from the CD3ζ chain or the FcRIγ chain (15–18). The signaling function of CARs has been questioned based on findings in transgenic mice and transduced primary T cells, indicating that antigen ligation was not always sufficient to activate resting naïve mouse T cells (19) or elicit interleukin 2 (IL-2) secretion in retrovirally transduced human peripheral blood T cells (20). We and others subsequently showed that ζ chain–based CARs could induce strong activation capable of sustaining T-cell proliferation and permitting secondary antigenic restimulation *in vitro* provided that antigen was presented in the context of CD28-mediated costimulation (21–23). It is not known, however, whether T cells expanded in this manner, particularly human T cells, could mediate tumor eradication *in vivo*, and whether further *in vivo* costimulation would be needed to sustain their function.

Note: Supplementary data for this article are available at Cancer Research Online (http://cancerres.aacrjournals.org/).

T.P.F. Gade, W. Hassen, and E. Santos contributed equally to this work.

Requests for reprints: Michel Sadelain, Memorial Sloan-Kettering Cancer Center, 1275 York Avenue, New York, NY 10021. Phone: 212-639-6190; Fax: 917-432-2340; E-mail: m-sadelain@ski.mskcc.org.

©2005 American Association for Cancer Research.

doi:10.1158/0008-5472.CAN-05-0436

Downloaded from cancerres.aacrjournals.org on September 13, 2017. © 2005 American Association for Cancer Research.

Here, we investigate the *in vivo* function of Pz1, a CAR-targeting human PSMA. PSMA is a highly attractive target antigen that is found in most prostate cancer cells, including hormone refractory metastatic disease (24, 25). The Pz1 receptor encompasses the ζ chain of the CD3 complex as its activation domain and specifically redirects *in vitro* cytolysis against PSMA-positive tumor cell lines (20). To investigate whether expanded $Pz1^+$ T cells are active *in vivo* and require costimulation after adoptive transfer, we established three tumor models in severe combined immunodeficient (SCID)-*bg/bg* mice—orthotopic, s.c., and pulmonary. Direct administration of $Pz1^+$ T cells in orthotopic and s.c. human prostate tumors eliminated a majority of the tumors. In a systemic tumor model in which mice rapidly succumbed to pulmonary disease, i.v. administration of Pz1-transduced T cells induced objective responses in all mice and cured a substantial fraction of them. Altogether, our results strongly support the feasibility of targeting prostate cancer with autologous T lymphocytes directed against PSMA by a transduced ζ chain–based receptor.

Materials and Methods

Cell Lines

Retroviral producer cells were maintained in DMEM (Invitrogen, Carlsbad, CA) supplemented with 10% FCS. LNCaP and LNCaP/B7 cells were maintained in RPMI (Invitrogen) with 10% fetal bovine serum (FBS; Hyclone, Logan, UT). NIH3T3 fibroblasts (American Type Culture Collection, Rockville, MD) were maintained in DMEM with 10% donor calf serum (Hyclone). RM1, RM1.PGLS, and EL4 were grown in high-glucose DMEM supplemented with sodium pyruvate, 10% FBS, and 2 mmol/L glutamine (Invitrogen). All media contained penicillin (100 units/mL) and streptomycin (100 μg/mL).

Vectors

The oncoretroviral vectors encoding Pz1, human PSMA, 19z1, and CD80/B7.1 are described (20, 23, 26). SFG-Egfp/Luc was generated by subcloning the fusion gene coding sequence from pEGFPluc (BD Biosciences, San Jose, CA) into the *Nco*I and *Bam*HI restriction sites of SFG, a variant of MFG.S (27).

Peripheral Blood Lymphocyte Collection and Retroviral Transduction

An average volume of 100 mL peripheral blood was drawn from healthy donors with informed consent. Peripheral blood mononuclear cells were isolated with Accu-Prep Lymphocytes (Accurate Chemical and Scientific Company, Westbury, NY) by low-density centrifugation and cultured in RPMI 1640 and seeded at a density of 2×10^6/mL with 1 μg/mL phytohemmaglutinin. After 48 hours, T cells were exposed to gibbon ape leukemia virus envelope-pseudotyped Pz1 or 19z1 vector as previously described (20, 23, 26).

$Pz1^+$ T-cell Expansion

LNCaP cells were transduced with the SFG-CD80 vector (20) and sorted based on CD80 expression. The sorted cells, termed LNCaP/B7, were found to stably express CD80, obviating the need to periodically repurify CD80-expressing cells. Three days after peripheral blood lymphocyte (PBL) transduction, $Pz1^+$ T cells were expanded on LNCaP/B7 cells in six-well tissue culture plates in the presence of 50 units/mL IL-2 (supplemented every 2-3 days). This cycle was done once before adoptive transfer or repeated on day 7 for *in vitro* restimulation studies. $19z1^+$ T cells were expanded on fibroblast-derived artificial antigen-presenting cells expressing CD19 and CD80 as described (26).

Cytotoxicity Assays

Transduced T-cell effector function was measured in standard ^{51}Cr release assays using EL4, $EL4^{PSMA}$ (23), RM1, RM1.PGLS, and LNCaP as targets. The T cells were incubated with ^{51}Cr-labeled target cells for either 4 or 12 hours. Specific ^{51}Cr release was calculated using the following formula: percentage of specific lysis = [(cpm experimental release − cpm spontaneous release) / (cpm maximum release − cpm spontaneous release)] × 100. The SD of triplicates was in all cases <5%. The effector-to-target cell ratio was based on the determination of $CD8^+$ $Pz1^+$ or $CD8^+$ $19z1^+$ T cells by fluorescence-activated cell sorting (FACS) analysis. For the antibody blocking experiment, targets cells were preincubated for 30 minutes (24–26) with 10 μg/10^6 cells of anti-MHC class I (clone W6/32; Axxora, San Diego, CA) or purified mouse IgG1 as control.

Flow Cytometry

Expanded PBLs were stained for the expression of differentiation markers immediately before injection into SCID beige mice. Pz1 and 19z1 cell surface expression was measured using a cross-reactive goat anti-mouse IgG phycoerythrin conjugate (CN Biosciences, La Jolla, CA). The following antibodies were used for subset identification: anti-CD8-APC, anti-CD27-phycoerythrin (PE), anti-CD4-APC, anti-CD4-PE-Cy5, anti-CD28-PE (Caltag, La Jolla, CA), anti-CCR7-PE (R&D Systems, Minneapolis, MN), and anti CD45RA-PE-Cy5 (eBioscience, San Diego, CA), and, as isotype controls, PE-conjugated mouse IgG2b (BD Biosciences) or mouse IgG1-PE. Intracellular perforin expression was assessed after fixation with CYTOFIX buffer and permeabilized with PERM/WASH buffer (both from BD Biosciences) using a PE-conjugated mouse anti-human perforin monoclonal antibody (mAb; BD Biosciences).

Mouse Models

Orthotopic surgery. Male SCID beige mice between 5 and 8 weeks old (Taconic, Haverford, NY) were anesthetized with i.p. injection of ketamine and xylazine solution. The dorsolateral aspect of the prostate was injected with 1×10^6 LNCaP cells in 25 μL RPMI + 10% FCS solution. Tumors were allowed to grow for 10 days to 3 weeks before injection with T cells. Serum PSA-positive mice were randomized to receive either Pz1 or 19z1 cells. Pz1 and 19z1-transduced T cells were injected directly into the prostate tumors at equal doses of 20×10^6 total T cells (6-8 million $CD8^+$ $Pz1^+$ T cells) given in two injections over 48 hours. Mice were then followed until death or sacrificed if they showed any signs of distress, as determined by an independent observer.

Subcutaneous model. One million LNCaP/C4-2 cells were injected s.c. Mice were sacrificed when the tumors reached a volume of 1 cm^3.

Lung model. Five thousand RM1.PGLS cells were administered i.v. on day 0. The RM1 cells were retrovirally transduced to express human PSMA and Egfp/Luc and sorted to high purity (99% $PSMA^+$, $Egfp/Luc^+$). $Pz1^+$ $CD8^+$ PBLs (5×10^6-8×10^6) were administered i.v. at 24, 48, and 72 hours after tumor injection. For the 1:10 ratio (Pz1:19z1) experiment (Fig. 5*C*), we injected i.v. 20×10^6 19z1 T cells on days −2, −1, 4, and 5; 10×10^6 19z1 and 5×10^6 $CD8^+$ $Pz1^+$ T cells on days 1 and 2; and 5,000 RM1.PGLS cells were administered i.v. on day 0.

Lung T-cell retrieval. Single cell suspensions of tissues from sacrificed animals were made by macerating tissues through a 40 μm nylon cell strainer (Becton Dickinson, Franklin Lakes, NJ). Isolated cells were analyzed by FACS for expression of human CD3 and CD45 using PE-labeled anti-human CD3 and FITC-labeled anti-human CD45 mAbs (Caltag).

Magnetic Resonance Imaging

Orthotopic model. Mice selected at random from the two treatment groups were anesthetized with a single i.p. injection of ketamine (90 mg/kg) and xylazine (9 mg/kg). Thirteen to 15 mice were then positioned together within a custom-built three-turn parallel wound foil solenoid. The studies were done on a GE Signa 1.5 T clinical scanner (GE Medical Systems, Milwaukee, WI) operating at 63.9 MHz. Axial prostate images were acquired using a fast spin echo imaging sequence with repetition time (TR) of 5,000 milliseconds, echo time (TE) of 102 milliseconds, number of excitations (NEX) of 4, field of view (FOV) of 8 × 8 cm, slice thickness of 1.5 mm, slice gap of 0.5 mm, matrix size of 512 × 256, and in-plane resolution of 156 × 312 μm. Tumor volumes were calculated using the GE Advantage Workstation 4.0_03 software.

Lung model. Two mice from each group were selected at random for magnetic resonance imaging (MRI) on days 7 and 13 posttumor inoculation. Each mouse was anesthetized using 2% isoflurane (Forane, Baxter Healthcare Corp, Deerfield, IL) and positioned within a four-turn parallel wound foil solenoid. These studies were also done on a GE Signa 1.5 T

Downloaded from cancerres.aacrjournals.org on September 13, 2017. © 2005 American Association for Cancer Research.

clinical scanner. Axial images were acquired using a spoiled gradient echo sequence with TR = 100 milliseconds, TE = 6.3 milliseconds, flip angle = 20°, NEX = 14, FOV = 4 × 4 cm, slice thickness = 1.0 mm, slice gap = 1.5 mm, matrix size = 256 × 192. To better quantify tumor burden and distribution at day 7, a mouse was positioned within a Bruker Biospec spectrometer (Bruker, Billerica, MA) operating at 7.05T. Contiguous axial images were acquired using a birdcage coil and a spoiled gradient echo sequence with TR = 179 milliseconds, TE = 5.2 milliseconds, flip angle = 30°, NEX = 48, FOV = 3 × 3 cm, slice thickness = 0.8 mm, slice gap = 1 mm, matrix size = 256 × 256. The tumor volumes were quantified using Bruker Paravision 3.0.1 software.

Microcomputed Tomography Imaging

Noncontrast small-animal X-ray computed tomography (CT) imaging was done using the MicroCAT II scanner (ImTek, Inc., Knoxville, TN), with an X-ray source having a 50 μm tungsten anode and operated at 55 kVp and 800 μA and a phosphor detector optically coupled to a 1,820 × 3,488 charge-coupled device. A total of 360 conebeam projections were acquired with an exposure time of 750 milliseconds each. Images were reconstructed three-dimensionally in a 512 × 512 × 1,024 matrix using the Feldkamp conebeam filtered back-projection algorithm. Total CT acquisition time was ~10 minutes and the spatial resolution (full-width half-maximum) was 100 μm. Visualization and analyses of CT images were done using the Amira (Konrad-Zuse-Zentrum fürInformationstechnik Berlin and Indeed Visual Concepts GmbH) software.

Immunohistochemistry

Fresh tissue samples were embedded in optimal cutting temperature compound and frozen in isopentane cooled in liquid nitrogen before storing at −70°C. Sections of 8 to 10 μm were cut on a cryostat at −20°C. The sections were laid onto Vectobond slides (Sigma, St. Louis, MO) and dried in air for 15 minutes. The sections were fixed in cold acetone for 2 minutes and then immersed in 0.3% hydrogen peroxide in 0.1% (w/v) sodium azide for 10 minutes. Slides were washed with PBS and incubated with 5% bovine serum albumin (BSA) in PBS for 60 minutes at room temperature. Following the removal of BSA, 5 μg/mL of anti-PSMA J591 mAb* (generously provided by Dr. Neil Bander, Weill Medical College of Cornell University) was applied followed by thorough washing with PBS before application of horseradish peroxidase-conjugated goat anti-human IgG mAb (Jackson Immunoresearch, West Grove, PA) at a 1:1,000 dilution for 60 minutes. After washing with PBS, 0.06% diaminobenzidine tetrachloride and 0.01% hydrogen peroxide in PBS were applied onto the specimens for 3 minutes. The sections were then washed, lightly stained with Carazzi's hematoxylin, dehydrated, and mounted.

Quantitative Bioluminescence

Bioluminescence images were collected on a Xenogen IVIS Imaging System (Xenogen, Alameda, CA) using a cryogenically cooled charge-coupled device camera. Living Image software (Xenogen) was used to acquire and quantitate the bioluminescence imaging data sets. Ten to 15 minutes before the time of imaging, a single i.p. injection of 150 mg/kg D-luciferin (Xenogen) in PBS was administered to each mouse. Subsequently, the animals were induced using 2% isoflurane (Forane, Baxter Healthcare) and positioned within the imaging chamber under anesthesia. Two to five mice were imaged simultaneously with exposure times ranging from 0.5 to 3 minutes. Ten, 15, or 25 cm field of view and low, medium, or high binning levels were applied to maximize sensitivity and spatial resolution. Both dorsal and ventral images were obtained for each animal. The dorsal and ventral signals were separately quantified through region of interest (ROI) analysis over the thoracic region. The resulting signal summations (in units of photons/s) were normalized to the ROI area so that all measurements are given in photons/s/cm^2. For each image, normalized background signal from similarly sized ROIs was subtracted.

Statistics

Statistical analyses and curve fittings were done using GraphPad Prism version 4.00 for Windows (GraphPad Software, San Diego, CA). Survival curves were created using the product limit method of Kaplan and Meier and compared using the log-rank test. Linear regression analysis was used to fit the quantitated bioluminescence data to the FACS-determined tumor cell counts, whereas nonlinear regression analysis was used to fit the quantitated bioluminescence data to the FACS-determined T-cell counts.

Results

Specific expansion of prostate-specific membrane antigen–specific primary T lymphocytes. We previously showed that Pz1-transduced human primary T cells efficiently lyse PSMA-positive target cells *in vitro*, including LNCaP cells and PSMA-transduced PC3 cells, EL4 cells, and NIH 3T3 fibroblasts (20, 23). However, these Pz1$^+$ PBLs failed to expand in response to repeated antigenic stimulation in the absence of CD28-mediated costimulation (23). As shown in Supplementary Fig. S1*A*, Pz1-transduced PBLs likewise failed to sustain proliferation in the presence of LNCaP cells, but expanded 8 to 10-fold in a single round of *in vitro* stimulation with CD80/B7.1-expressing LNCaP cells (LNCaP/B7). Both CD4$^+$ and CD8$^+$ Pz1 T cells present in these PBL cultures expanded, starting from a 2:1 ratio and typically reaching a 1:2 ratio by day 14. When cultured separately, the CD4$^+$ Pz1$^+$ T cells expanded in response to PSMA + CD80 in two consecutive stimulations, but not the CD8$^+$ Pz1$^+$ T cells, which showed diminished expansion upon restimulation despite the addition of exogenous IL-2 (Supplementary Fig. S1*B*). Thus, absolute expansion was consistently the highest when CD4 and CD8 T cells were cocultured in the presence of PSMA and CD80. For the *in vivo* studies shown below, the transduced PBLs were exposed once to LNCaP/B7 cells before adoptive transfer. T cells expanded in this manner were highly specific for xenogeneic PSMA+ tumor cells and efficiently lysed hematopoietic and epithelial mouse tumor cells expressing human PSMA (Fig. 1*A-C*). Pz1$^+$ T cells also lysed LNCaP cells (Fig. 1*D*). Lysis of LNCaP cells was not reduced in the presence of blocking antibody against HLA class I (Supplementary Fig. 1*D*), indicating that alloreactivity did not significantly contribute to target cell recognition and further demonstrating that tumor cell lysis occurred in an HLA-independent manner. T cells transduced with a control CAR specific for CD19 showed little or no cytotoxic activity against the same target cells (Fig. 1).

Expanded Pz1$^+$ T cells comprise activated and effector memory T cells. Based on their cell surface phenotype, CD8$^+$ T cells can be assigned to five distinct differentiation stages (28): naïve (CCR7$^+$; CD45RA$^+$), central memory (T_{CM}; CCR7$^+$; CD45RA$^-$), early effector T cells (CCR7$^-$; CD45RA$^-$; CD28$^+$); effector memory T cells (T_{EM}; CCR7$^-$; CD45RA$^-$; CD28$^-$); and CD45RA$^+$ effector memory cells (T_{EMRA}; CCR7$^-$; CD45RA$^+$, CD28$^-$). The expanded Pz1$^+$ CD8$^+$ T cells were characterized on the day of injection, typically 5 to 7 days after initiating cocultivation with LNCaP/B7 cells. The vast majority of the Pz1$^+$ CD8$^+$ T-cell population was CCR7$^-$ CD45RA$^-$, about half of which were positive for CD28, thus corresponding to early effector and effector memory phenotypes, respectively (Supplementary Fig. S2*A-C*). The expanded Pz1$^+$ T cells markedly up-regulated perforin expression compared with untransduced T cells (Supplementary Fig. S2*D*), consistent with their high lytic potential (Fig. 1).

Pz1$^+$ peripheral blood lymphocytes eradicate established orthotopic LNCaP tumors. To assess the *in vivo* function of Pz1-transduced human PBLs, we first established an orthotopic model using the PSA-secreting prostate adenocarcinoma cell line LNCaP.C4-2 (29). Following surgical implantation of 1 million cells, PSA serum levels and tumor size were monitored by RIA and MRI, respectively. The tumors were ~0.02 to 0.03 cm^3 when serum PSA became unequivocally positive (>0.01 ng/mL) and increased to a median value of 0.75 cm^3 within 5 weeks, by which time tumor-bearing animals had to be sacrificed. The correlation between tumor weight estimated by MRI and tumor weight measured after necropsy was linear (r^2 = 0.96, P = 0.002). Ten days after tumor

Downloaded from cancerres.aacrjournals.org on September 13, 2017. © 2005 American Association for Cancer Research.

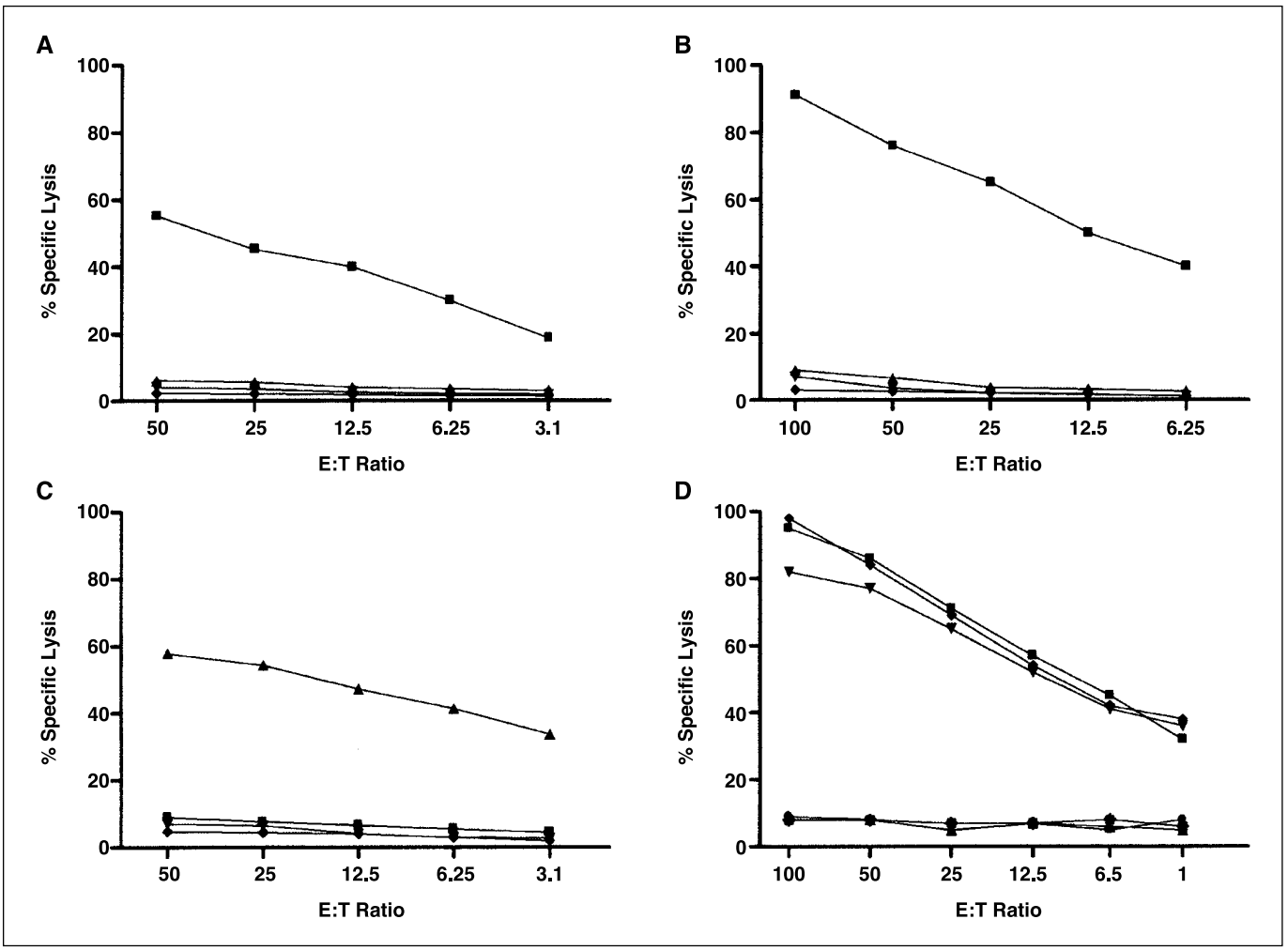

Figure 1. *In vitro* cytolytic activity of Pz1-transduced PBLs. Target cell lysis by Pz1-redirected PBLs. T cells transduced with either Pz1 or 19z1 as control were assayed 5 days after stimulation with LNcaP/B7.1 or 3T3 CD19/B7.1 cells, respectively. The target cells included RM1.PGLS and RM1 (*A* and *B*), EL4^{PSMA} and EL4 (*C*) and LNCaP (*D*). The Pz1$^+$ T cells efficiently lysed PSMA$^+$ target cells (20, 23), but not the 19z1$^+$ PBLs, neither after 4 hours (*A, C, D*) nor after 12 hours (*B*). Pz1$^+$ T cells did not lyse PSMA-negative targets. Data are representative of five independent experiments done at the time of T-cell infusion in adoptive transfer experiments. *A* and *B,* ■ Pz1$^+$, target: RM1.PGLS; ▲ Pz1$^+$, target: RM1; ♦ 19z1$^+$, target: RM1.PGLS; ▼ 19z1$^+$, target: RM1. *C,* ■ Pz1$^+$, target: EL4; ▲ Pz1$^+$, target: EL4^{PSMA}; ♦ 19z1$^+$, target: EL4; ▼ 19z1$^+$, target: EL4^{PSMA}; *D,* ■ Pz1$^+$, target: LNCaP; ♦ Pz1$^+$, target: LNCaP + isotype control; ▼ Pz1$^+$, target: LNCaP + W6/32; ▲ 19z1$^+$, target: LNCaP; ★ 19z1$^+$, target: LNCaP + isotype control; ● 19z1$^+$, target: LNCaP + W6/32.

inoculation, serum PSA-positive mice were randomized to two treatment groups, receiving either Pz1 or control 19z1-transduced PBLs. Ten million transduced PBLs were administered locally on days 11 and 12 after tumor implantation. Fifty-four mice were treated (n = 26 for Pz1 and n = 28 for 19z1). In half of the mice, tumor progression was followed weekly by MRI (Fig. 2*A* and *B*). The median survival in the Pz1 group was 211 days (range 28-272 days), in contrast to 53 days in the 19z1 group (range 23-147 days; $P < 0.0001$). Fifteen mice treated with Pz1-transduced PBLs (57%) remained without evidence of disease by the end of the study on day 272, which was corroborated by absence of detectable serum PSA (data not shown) and by MRI. No mouse survived in the 19z1 control group (Fig. 2*C*). The 19z1-treated animals showed the same growth rate as untreated mice (data not shown). Interestingly, the tumors in Pz1-treated mice initially showed modest growth, reaching 0.08 cm^3 on average (range 0.01-0.6 by day 18) followed by shrinkage and tumor elimination in the long-term survivors.

Pz1-transduced peripheral blood lymphocytes eradicate established s.c. LNCaP tumors. To test T-cell efficacy at other tumor sites and assess the tumor response in relation to tumor size, we established a s.c. tumor model. Serum PSA was detectable 7 to 14 days after implantation of 5 × 10^5 LNCaP/C4-2 cells and tumors were palpable by days 10 to 14. As in the orthotopic model, the relationship between serum PSA and tumor volume was linear 15 and 30 days after tumor implantation (data not shown).

A first set of 22 mice with an average tumor size of 0.07 cm^3 (mean PSA, 1.7 ng/mL) was treated with 10 million human PBLs (either Pz1 transduced or untransduced) by direct intratumoral injection on 2 consecutive days. The tumors progressed to >1 cm^3 in 11 of 11 mice treated with control PBLs, correlating with a rapid rise in serum PSA. In contrast, the tumors were successfully eradicated in 6 of 11 (55%) of the mice receiving Pz1-transduced lymphocytes as evidenced by impalpable tumor and undetectable serum PSA for at least 180 days ($P < 0.0001$; Fig. 3*A*). Moreover, the tumors remaining at day 60 in the Pz1$^+$ T cell–treated mice were smaller than the tumors in the control cohort (mean 0.23 versus 1.61 cm^3, P = 0.02).

Downloaded from cancerres.aacrjournals.org on September 13, 2017. © 2005 American Association for Cancer Research.

A second set of animals with a larger tumor burden (mean size, 0.28 cm^3; mean PSA, 3.6 ng/mL) was treated with the same T-cell dose (n = 8 with $Pz1^+$ PBLs and n = 8 with mock transduced PBLs). Half (four of eight) of the established tumors were eradicated by the Pz1-transduced T cells, remaining free from both local and systemic recurrence for at least 180 days, whereas none of the eight tumors were eradicated by the control T cells (P = 0.0043; Fig. 3*B*).

Systemically administered $Pz1^+$ peripheral blood lymphocytes can eradicate pulmonary tumors. To investigate the bioactivity of systemically delivered T cells, we established a lung metastasis model. The murine prostate cell line RM1 (30) was retrovirally transduced to express human PSMA as well as the GFP/Luciferase fusion protein (RM1.PGLS) to facilitate tumor tracking and the quantification of tumor burden. RM1.PGLS cells were detectable in the lung within 24 hours of i.v. administration and remained localized in the lung parenchyma, developing as nodules detectable by MRI and CT scan within 7 days (Fig. 4*A*). The tumors gradually invaded the lung parenchyma, causing major airway obstruction by day 13, at which time the animals were sacrificed (Fig. 4*B*). T cells transduced with either Pz1 or 19z1 were infused i.v. on days 1, 2, and 3 at a dose of 5×10^6 to 8×10^6 transduced PBLs per day. All mice treated with Pz1 (n = 16) responded to treatment (Fig. 5*A*). One third remained tumor-free (survival >90 days without evidence of tumor), whereas the others showed significantly delayed tumor progression (mean survival time doubling from 12 to 23 days; Fig. 5*A*). Control $19z1^+$ T cells did not delay tumor progression relative to untreated mice (Fig. 5*A*), underscoring the specificity imparted by the CAR. Conversely, $Pz1^+$ T cells were without effect on $PSMA^-$, $CD19^+$ Raji cells, which in turn were eliminated by the 19z1-transduced T cells (Fig. 5*B*). To assess whether the lymphodepleted milieu of the recipient SCID mice facilitated tumor eradication by $Pz1^+$ T cells, we did an additional experiment in which mice received either $Pz1^+$ T cells or $Pz1^+$ T cells plus $19z1^+$ T cells at a 1:10 ratio. As shown in Fig. 5*C*, there was no significant survival difference between mice treated with Pz1 T cells (n = 8) and mice treated with Pz1 T cells and 19z1 T cells (n = 12; Fig. 5*C*). No tumor was detectable by quantitative bioluminescence in long-term survivors with Pz1 T cells or $Pz1^+$19z1 T cells (data not shown).

Prostate-specific membrane antigen–specific T cells take over a week to eradicate established tumors. To analyze the kinetics of tumor elimination, we measured tumor progression by quantitative bioluminescence in all Pz1-treated mice (n = 16),

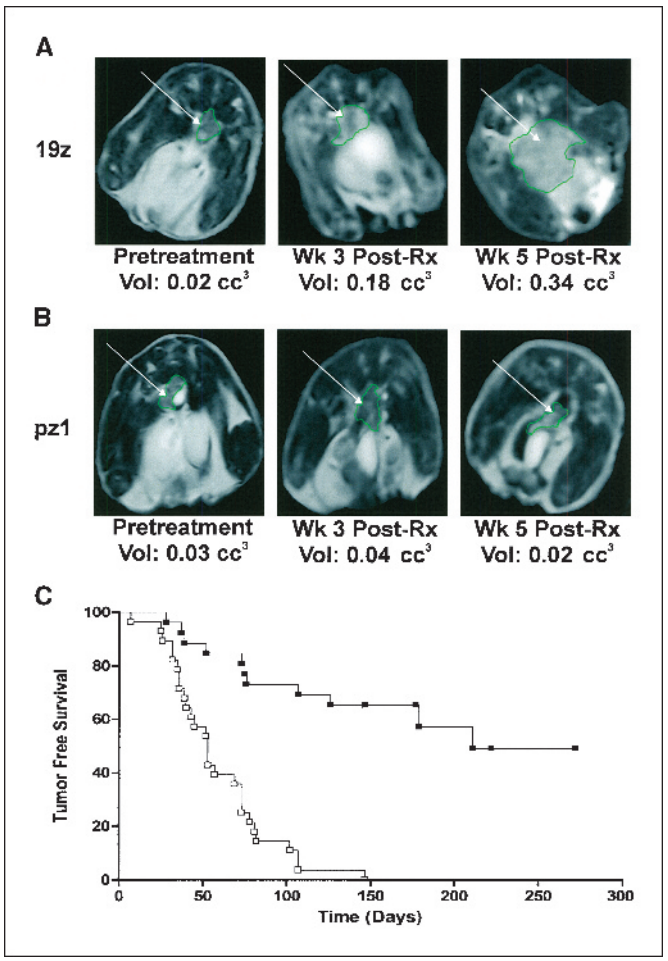

Figure 2. Orthotopic tumor model. MRI and survival data. *A,* representative control animal (treated with $19z1^+$ T cells) showing progressive tumor growth. *B,* representative example of an animal cured by $Pz1^+$ PBLs. Median prostate volumes: pretreatment 0.03 cm^3; 19z1-treated 0.18 and 0.75 cm^3, 3 and 5 weeks posttherapy, respectively; pz1-treated 0.08 and 0.03 cm^3, at the same time points. *C,* orthotopic model: survival after local $Pz1^+$ T-cell administration. Mice with established tumors (serum PSA, magnetic resonance) were randomized in two treatment groups and received either $Pz1^+$ PBLs (n = 26, ■) or control T cells from the same donors, but transduced with the 19z1 receptor (n = 28, □).

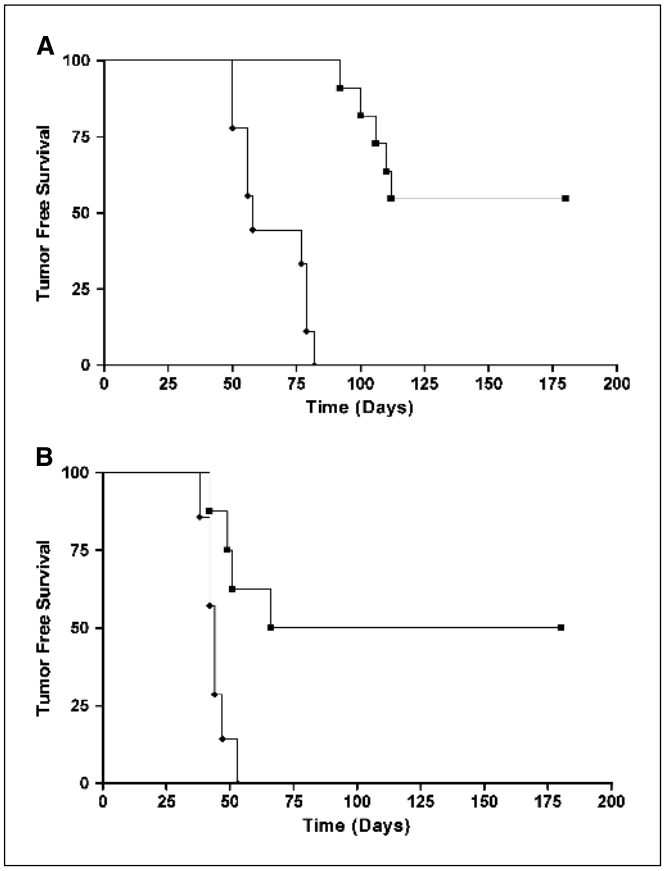

Figure 3. S.c. model. Survival after local $Pz1^+$ PBL administration. *A,* tumor-free survival after T-cell infusion in tumors averaging 0.04 cm^3. Pz1: n = 11, ■; control: n = 11, ◆. *B,* tumor-free survival after T-cell infusion in tumors averaging 0.28 cm^3. Pz1: n = 8, ■; control: n = 8, ◆.

Downloaded from cancerres.aacrjournals.org on September 13, 2017. © 2005 American Association for Cancer Research.

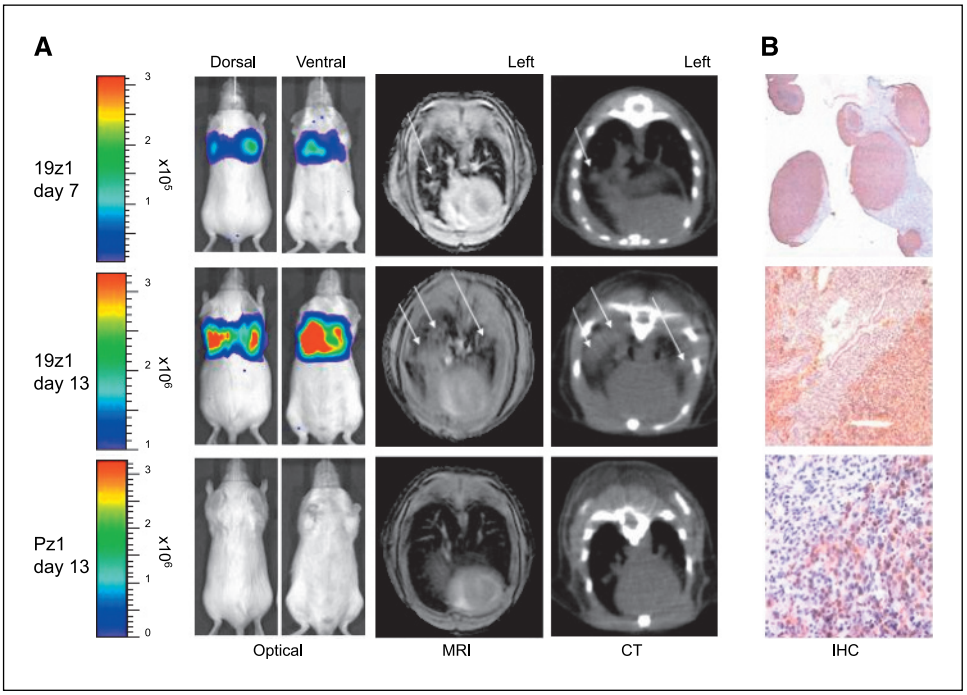

Figure 4. RM1.PGLS lung model. Characterization by bioluminescence imaging, MRI, CT, and immunohistochemistry (*IHC*). *A,* bioluminescence imaging, MRI, and CT in control mice, which show the very aggressive progression of RM1.PGLS 7 and 13 days after tumor infusion. A representative animal cured by Pz1$^+$ PBLs is also shown (day 13 bioluminescence imaging, MRI, and CT). The lung optical signals correlated well with the nodular lesions (*arrows*) seen in both CT and MRI studies. The RM1.PGLS tumors remain exclusively in the lung. *B,* immunohistochemistry showing nodular lung tumors, positive for human PSMA expression (day 13 after tumor infusion). Normal lung tissue stained negative (data not shown). Magnifications, ×4, ×10, and ×40.

as well as 19z1-treated mice (n = 9) and untreated mice (no T cells, n = 8). Tumor progression was indistinguishable between the two latter groups (Fig. 6), indicating that non-PSMA targeted T cells had no effect on the tumor. Eleven of the Pz1-treated mice showed partial responses or complete remission followed by relapse (Fig. 6*A*). Of these, two were negative in two consecutive imaging sessions (days 10 and 13), followed by delayed, fatal tumor progression. Examination of lung tissue by immunohistochemistry showed that the progressing tumors remained by and large positive for PSMA, thus excluding antigen down-regulation as the mechanism of tumor escape. Importantly, we found that mice brought into transient complete remission (n = 2; Fig. 6*A*) as well as mice eventually cured by Pz1 treatment (n = 5; Fig. 6*B*) showed continued tumor progression in the 3 to 10 days following T-cell administration before tumors started regressing. These data established that the T cells were not immediately effective and implied that therapeutic T cells must persist for at least 1 week to eradicate the tumor. This conclusion was further supported by measuring residual T-cell numbers in mice responding to therapy. We enumerated lung T cells and quantified tumor mass in seven mice treated with Pz1$^+$ T cells at day 17, by which time all control mice had succumbed to their disease. As shown in Fig. 6*C* and *D*, there was a strong inverse correlation between T-cell count and tumor, thus confirming the direct relationship between *in vivo* T-cell persistence and tumor rejection.

Discussion

Our results show that Pz1-transduced PBLs are highly antigen specific and cytolytic *in vivo*. In three tumor models—orthotopic, s.c., and lung metastases—we show that Pz1 but not 19z1-transduced T cells induce durable remissions and cures in a substantial fraction of the treated animals. In all of our experiments, mice with orthotopic (n = 26), s.c. (n = 19), or pulmonary tumors (n = 16) received a total of 18 to 20 million Pz1$^+$ T cells administered in either two (Figs. 2 and 3) or three (Figs. 4 and 5) consecutive injections. Complete responses and long-term survival were achieved in 55% of the direct infusions in prostate or skin (n = 45). In the partial responders, survival was extended up to 200 days in mice with orthotopic tumors (average tumor size of 0.02 cm^3; Fig. 2), to 110 days in mice with 0.04 cm^3 s.c. tumors (Fig. 3*A*), and to 65 days in mice with 0.28 cm^3 s.c. tumors (Fig. 3*B*). These results indicate that the therapeutic response rate is proportional to the intratumoral effector-to-target cell ratio.

Significantly, Pz1-transduced human T cells could not engage their endogenous T-cell receptor when recognizing PSMA on RM1.PGLS cells, thus excluding any role for the endogenous T-cell receptor and establishing that tumor elimination was strictly mediated by the Pz1 receptor. The 19z1$^+$ T cells had no effect on tumor progression in prostate or in lung, which underscores the targeting specificity afforded by Pz1 and excludes nonspecific inflammation as a mechanism sufficient to account for tumor regression, thus further underscoring the targeting specificity afforded by Pz1.

Antigen-induced *ex vivo* expansion of the transduced cells required costimulation, which was provided here by expressing CD80 in LNCaP tumor cells (Fig. 1). A critical question for immunotherapy is whether adoptively transferred T cells require *in vivo* costimulation to achieve tumor protection. This important question is difficult to assess because of the difficulty of pinpointing whether the infused T cells interact with antigen cross-presented by dendritic cells or other antigen-presenting cells at any time before their contact with the tumor, irrespective of the costimulatory ligands presented by the latter (31–34). Here, we took advantage of non–MHC-restricted antigen recognition and a xenogeneic setting to address this question, establishing *in vivo* models in which cross-presented LNCaP antigens could not stimulate the Pz1 antigen receptor. To

Downloaded from cancerres.aacrjournals.org on September 13, 2017. © 2005 American Association for Cancer Research.

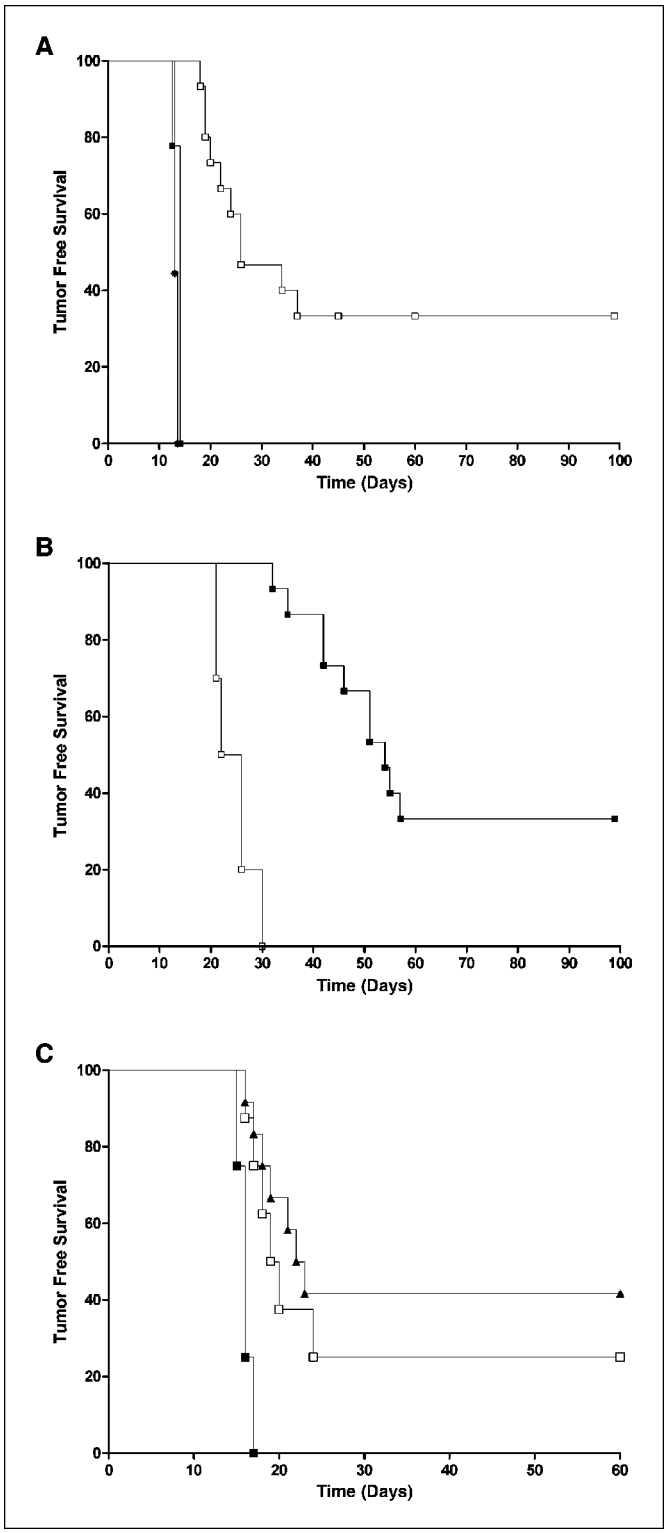

Figure 5. RM1.PGLS lung model. Survival after i.v. administration of Pz1- versus 19z1-transduced PBLs. *A,* RM1.PGLS lung model: $Pz1^+$ PBLs ($n = 16$, □), $19z1^+$ PBLs ($n = 9$, ■), or no treatment ($n = 8$, ●). Pz1-transduced T cells eliminate established RM1.PGLS, but not $19z1^+$ PBLs ($P < 0.0001$, Pz1 versus 19z1 or untransduced T cells). *B,* Raji medullary model (25): $Pz1^+$ PBLs ($n = 10$, □) and $19z1^+$ PBLs ($n = 20$, ■). 19z1-transduced T cells eliminate established Raji, but not $Pz1^+$ PBLs ($P < 0.0001$). *C,* RM1.PGLS lung model: $Pz1^+$ PBLs ($n = 8$, □), $Pz1^+$ PBLs in combination with a 1:10 ratio of $19z^+$ PBLs ($n = 12$, ▲) or $19z1^+$ PBLs ($n = 4$, ■). Survival is not statistically different between the two former groups.

address whether the "immunologic space" available in recipient SCID mice contributed to this therapeutic response, we did an experiment in which recipient mice were "filled" with a 10:1 excess of irrelevant $19z1^+$ T cells (100 million T cells per recipient, which alone had no effect on tumor progression). As shown in Fig. 5*C*, this massive infusion of nontargeted T cells did not reduce tumor eradication, establishing that $Pz1^+$ T cells were still fully effective under such competitive conditions.

Our results also show that the adoptively transferred T cells eliminated established tumor cells in the absence of *in vivo* costimulation, as shown by the eradication of parental (CD80-negative) LNCaP cells as well as nonhuman, PSMA-positive RM1.PGLS tumors. This finding thus establishes that human T cells redirected through a ζ chain–based CAR are able to mediate tumor rejection without further *in vivo* costimulation. This observation does not rule out a role for *in vivo* costimulation of adoptively transferred T cells in tumor eradication, but establishes that, if T cells are provided in sufficient numbers and if they are adequately activated *ex vivo* before infusion, further *in vivo* costimulation is not necessary. Costimulation may nonetheless be important to promote T-cell proliferation, survival, and/or memory formation (15), thereby increasing or sustaining the effector-to-tumor cell ratio.

We found that tumor elimination was indeed closely correlated with short-term T-cell persistence after T-cell transfer. Quantitative bioluminescence imaging was used to monitor tumor burden in the RMI.PGLS lung model. Serial imaging studies showed that the tumors decreased to undetectable levels within 7 days in 7 of 16 Pz1-treated mice (Fig. 6). Among these seven complete responders, five mice showed continued tumor progression over the course of 1 week following the last T-cell infusion. This finding establishes that the therapeutic impact of T cells is neither immediate nor even very rapid, and further implies that, in this model, the T cells have to survive and remain functional for at least 7 days to exert their therapeutic effect. This time lag may represent a period during which tumor-specific T cells expand until a sufficient effector-to-target cell ratio is reached, or, alternatively, the period needed for T cells to recirculate and gradually reach each and every tumor site, which is required to achieve a cure. Two of seven mice in complete remission relapsed and showed progressive disease by day 18 after having scored negative on at least two consecutive imaging sessions on days 10 to 14 (Fig. 6*A*). Collectively, our measurements of tumor progression (Fig. 6) and correlation of T-cell count and tumor burden suggest that the T cells eliminated most, but not all, of the tumor cells by day 10 in these two animals and that the number of remaining T-cells did not impede subsequent tumor relapse from minimal disease because of an insufficient T cell-to-tumor ratio.

There is presently no effective treatment for disseminated prostate cancer. Approximately 25% of newly diagnosed prostate cancer cases present with metastatic disease (35) and 30% to 50% of patients who undergo definitive therapy for prostate cancer will show evidence of metastatic disease (36). Metastatic prostate cancer involves the bone and lung in over 90% and 46% of cases, respectively. Other frequent sites of metastases include the liver, pleura, and adrenal glands (37). Whereas metastatic disease is initially hormone sensitive, the natural history is progression to a hormone refractory state where the median survival is 12 to 18 months (38). Current systemic therapies have limited impact on survival (37).

Downloaded from cancerres.aacrjournals.org on September 13, 2017. © 2005 American Association for Cancer Research.

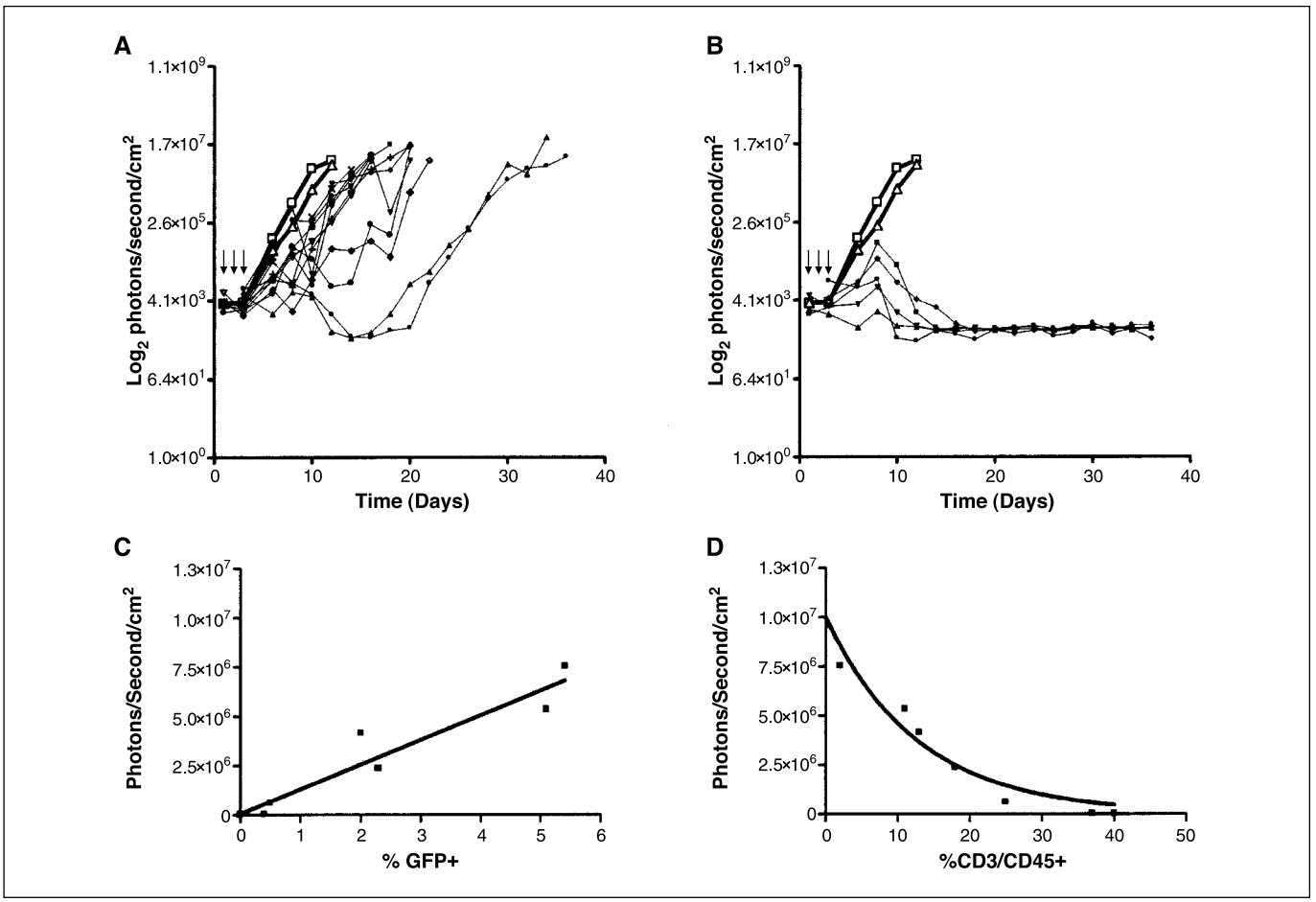

Figure 6. Quantitative bioluminescence analysis of tumor response to PSMA-targeted adoptive T-cell therapy. In (*A* and *B*), the two thick lines represent the mean thoracic optical signal measured in mice receiving either no T cells or 19z1-transduced T cells (average of eight and nine mice, respectively; the SDs are very small and not apparent). All other lines represent serial imaging in single mice treated with Pz1 T cells. In (*A*), partial or complete responder mice that rapidly progressed or relapsed after complete remission (n = 11). In (*B*), quantitative bioluminescence imaging in five mice that were ultimately cured by $Pz1^+$ PBLs (see Fig. 5). In several mice, continued tumor progression was noted in the imaging sessions following the T-cell infusions (*vertical arrows*), before the tumors eventually began regressing. In (*C*) and (*D*), T-cell and tumor cell counts were obtained by FACS assays done on whole lungs removed from another set of seven animals immediately following bioluminescence imaging on day 17. Regression analyses of bioluminescence tumor signal intensity versus lung RM1.PGLS tumor counts or lung $Pz1^+$ T-cell counts are shown in (*C*) and (*D*), respectively. *C,* linear relationship between bioluminescence imaging signal intensity and the number of tumor cells found in the lung 16 to 17 days after the injection of RM1.PGLS cells (y = 4.2e4 + 1.25e6x, r^2 = 0.92). *D,* decreasing monoexponential relationship between bioluminescence imaging signal intensity and the relative number of Pz1 receptor–positive T cells found in the lung at the same time points [y = 1e7exp(−0.077x), r^2 = 0.93].

Our studies show that Pz1 T cells are highly specific for PSMA and capable of mediating tumor elimination *in vivo*. Having established an efficacious method for expanding functional, PSMA-specific human T cells, we show antitumor function in three tumor models, including a systemic disease model. The data presented here establish that genetically modified human T cells targeted against PSMA not only suppress tumor growth, but markedly increase long-term survival. The genetic targeting of T cells is a strategy designed to rapidly generate populations of tumor-specific T lymphocytes (15–18). T cells may be engineered with physiologic T-cell receptors that are HLA-restricted or CARs that recognize cell surface antigens independent of HLA, as we do here. This latter approach is attractive for its potential applicability to any patient, irrespective of HLA haplotype, but is restricted to cell surface antigens. These include carcinoembryonic antigen (39), folate-binding protein (40, 41), erbB2-3-4 (42, 43), and Tag-72 (44), which have been targeted *in vivo* by genetically modified murine T lymphocytes (reviewed in ref. 45). Human T cells were shown to mediate *in vivo* tumor elimination in two recent studies targeting s.c. (42, 46) or medullary prostate tumors (47). In another tumor model, in which tumors localize in the medullary cavity (26), we showed that CAR-modified T cells could effectively eliminate bone marrow tumors. In aggregate, our results show that CAR-modified T cells are active in prostate, skin, lung, and bone marrow. PSMA is an attractive target for novel therapeutic applications because it is expressed in all prostate cancers and its expression levels increase in more poorly differentiated prostate cancers, including hormone refractory disease. Bander et al. (48) recently reported on the targeting of metastatic prostate cancer with a radiolabeled PSMA-specific mAb. The J591 mAb was found to accurately target bone or soft tissue lesions in at least 94% of evaluable tumor sites. Toxicity was limited to dose-related, reversible myelosuppression thought to be secondary to the antibody radiolabel. No patients developed anti-idiotypic antibodies (49). Thus, whereas PSMA is also expressed in normal prostate, the kidney proximal tubule, and

Downloaded from cancerres.aacrjournals.org on September 13, 2017. © 2005 American Association for Cancer Research.

the jejunum brush border (25), and putatively in the central nervous system (50), no related toxicities have been observed following antibody therapy. PSMA targeting with the Pz1 receptor may thus be useful for directing activated T cells against advanced prostate cancer. Altogether, our findings strongly suggest that Pz1-transduced T cells will effectively target metastatic prostate cancer in man.

Acknowledgments

Received 2/8/2005; revised 6/23/2005; accepted 7/20/2005.

Grant support: NIH grants CA-59350, CA-92629, CA-86438, CA-95152, CA-83084, and CA-08748; Mr. William H. Goodwin and Mrs. Alice Goodwin and the Commonwealth Cancer Foundation for Research and the Experimental Therapeutics Center of Memorial Sloan-Kettering Cancer Center; and Golfers Against Cancer.

The costs of publication of this article were defrayed in part by the payment of page charges. This article must therefore be hereby marked *advertisement* in accordance with 18 U.S.C. Section 1734 solely to indicate this fact.

References

1. Jemal A, Tiwari RC, Murray T, et al. Cancer statistics, 2004. CA Cancer J Clin 2004;54:8–29.
2. Hull GW, Rabbani F, Abbas F, Wheeler TM, Kattan MW, Scardino PT. Cancer control with radical prostatectomy alone in 1,000 consecutive patients. J Urol 2002; 167:528–34.
3. Pollack A, Smith LG, von Eschenbach AC. External beam radiotherapy dose response characteristics of 1127 men with prostate cancer treated in the PSA era. Int J Radiat Oncol Biol Phys 2000;48:507–12.
4. Pound CR, Partin AW, Eisenberger MA, Chan DW, Pearson JD, Walsh PC. Natural history of progression after PSA elevation following radical prostatectomy. JAMA 1999;281:1591–7.
5. Pardoll D. Does the immune system see tumors as foreign or self? Annu Rev Immunol 2003;21:807–39.
6. Gilboa E. The makings of a tumor rejection antigen. Immunity 1999;11:263–70.
7. Cho HJ, Bhardwaj N. Against the self: dendritic cells versus cancer. APMIS 2003;111:805–17.
8. Heiser A, Coleman D, Dannull J, et al. Autologous dendritic cells transfected with prostate-specific antigen RNA stimulate CTL responses against metastatic prostate tumors. J Clin Invest 2002;109:409–17.
9. Wolchok JD, Gregor PD, Nordquist LT, Slovin SF, Scher HI. DNA vaccines: an active immunization strategy for prostate cancer. Semin Oncol 2003;30: 659–66.
10. McNeel DG, Nguyen LD, Disis ML. Identification of T helper epitopes from prostatic acid phosphatase. Cancer Res 2001;61:5161–7.
11. Correale P, Walmsley K, Zaremba S, Zhu M, Schlom J, Tsang KY. Generation of human cytolytic T lymphocyte lines directed against prostate-specific antigen (PSA) employing a PSA oligoepitope peptide. J Immunol 1998;161:3186–94.
12. Lu J, Celis E. Recognition of prostate tumor cells by cytotoxic T lymphocytes specific for prostate-specific membrane antigen. Cancer Res 2002;62: 5807–12.
13. Reiter RE, Gu Z, Watabe T, et al. Prostate stem cell antigen: a cell surface marker overexpressed in prostate cancer. Proc Natl Acad Sci U S A 1998;95:1735–40.
14. Marincola FM, Wang E, Herlyn M, Seliger B, Ferrone S. Tumors as elusive targets of T-cell-based active immunotherapy. Trends Immunol 2003;24:335–42.
15. Sadelain M, Riviere I, Brentjens R. Targeting tumours with genetically enhanced T lymphocytes. Nat Rev Cancer 2003;3:35–45.
16. Geiger TL, Jyothi MD. Development and application of receptor-modified T lymphocytes for adoptive immunotherapy. Transfus Med Rev 2001;15:21–34.
17. Eshhar Z, Waks T, Bendavid A, Schindler DG. Functional expression of chimeric receptor genes in human T cells. J Immunol Methods 2001;248:67–76.
18. Ma Q, Gonzalo-Daganzo RM, Junghans RP. Genetically engineered T cells as adoptive immunotherapy of cancer. Cancer Chemother Biol Response Modif 2002; 20:315–41.
19. Brocker T. Chimeric Fv-ζ or Fv-ϵ receptors are not sufficient to induce activation or cytokine production in peripheral T cells. Blood 2000;96:1999–2001.
20. Gong MC, Latouche JB, Krause A, Heston WD, Bander NH, Sadelain M. Cancer patient T cells genetically targeted to prostate-specific membrane antigen specifically lyse prostate cancer cells and release cytokines in response to prostate-specific membrane antigen. Neoplasia 1999;1:123–7.
21. Geiger TL, Nguyen P, Leitenberg D, Flavell RA. Integrated src kinase and costimulatory activity enhances signal transduction through single-chain chimeric receptors in T lymphocytes. Blood 2001;98: 2364–71.
22. Haynes NM, Trapani JA, Teng MW, et al. Rejection of syngeneic colon carcinoma by CTLs expressing single-chain antibody receptors codelivering CD28 costimulation. J Immunol 2002;169:5780–6.
23. Maher J, Brentjens RJ, Gunset G, Riviere I, Sadelain M. Human T-lymphocyte cytotoxicity and proliferation directed by a single chimeric TCRζ/CD28 receptor. Nat Biotechnol 2002;20:70–5.
24. Israeli RS, Powell CT, Corr JG, Fair WR, Heston WD. Expression of the prostate-specific membrane antigen. Cancer Res 1994;54:1807–11.
25. Gong MC, Chang SS, Watt F, et al. Overview of evolving strategies incorporating prostate-specific membrane antigen as target for therapy. Mol Urol 2000; 4:217–22, discussion 223.
26. Brentjens RJ, Latouche JB, Santos E, et al. Eradication of systemic B-cell tumors by genetically targeted human T lymphocytes co-stimulated by CD80 and interleukin-15. Nat Med 2003;9:279–86.
27. Riviere I, Brose K, Mulligan RC. Effects of retroviral vector design on expression of human adenosine deaminase in murine bone marrow transplant recipients engrafted with genetically modified cells. Proc Natl Acad Sci U S A 1995;92:6733–7.
28. Geginat J, Lanzavecchia A, Sallusto F. Proliferation and differentiation potential of human $CD8^+$ memory T-cell subsets in response to antigen or homeostatic cytokines. Blood 2003;101:4260–6.
29. O'Keefe DS, Uchida A, Bacich DJ, et al. Prostate-specific suicide gene therapy using the prostate-specific membrane antigen promoter and enhancer. Prostate 2000;45:149–57.
30. Baley PA, Yoshida K, Qian W, Sehgal I, Thompson TC. Progression to androgen insensitivity in a novel *in vitro* mouse model for prostate cancer. J Steroid Biochem Mol Biol 1995;52:403–13.
31. Townsend SE, Allison JP. Tumor rejection after direct costimulation of $CD8^+$ T cells by B7-transfected melanoma cells. Science 1993;259:368–70.
32. Bai XF, Bender J, Liu J, et al. Local costimulation reinvigorates tumor-specific cytolytic T lymphocytes for experimental therapy in mice with large tumor burdens. J Immunol 2001;167:3936–43.
33. Prilliman KR, Lemmens EE, Palioungas G, et al. Cutting edge: a crucial role for B7-CD28 in transmitting T help from APC to CTL. J Immunol 2002;169: 4094–7.
34. Ochsenbein AF, Sierro S, Odermatt B, et al. Roles of tumour localization, second signals and cross priming in cytotoxic T-cell induction. Nature 2001;411:1058–64.
35. Stanford JL, Stephenson RA, Coyle LM, et al. Prostate cancer trends 1973-1995, SEER Program. Bethesda (MD): National Cancer Institute; 1999.
36. Pound CR. Evaluation and treatment of men with biochemical prostate specific antigen recurrence following definitive therapy for clinically localized prostate cancer. Rev Urol 2001;3:72–84.
37. Bubendorf L, Schopfer A, Wagner U, et al. Metastatic patterns of prostate cancer: an autopsy study of 1,589 patients. Hum Pathol 2000;31:578–83.
38. Halabi S, Small EJ, Kantoff PW, et al. Prognostic model for predicting survival in men with hormone-refractory metastatic prostate cancer. J Clin Oncol 2003; 21:1232–7.
39. Haynes NM, Snook MB, Trapani JA, et al. Redirecting mouse CTL against colon carcinoma: superior signaling efficacy of single-chain variable domain chimeras containing TCR-ζ vs Fcϵ RI-γ. J Immunol 2001;166:182–7.
40. Kershaw MH, Westwood JA, Hwu P. Dual-specific T cells combine proliferation and antitumor activity. Nat Biotechnol 2002;20:1221–7.
41. Wang G, Chopra RK, Royal RE, Yang JC, Rosenberg SA, Hwu P. A T cell-independent antitumor response in mice with bone marrow cells retrovirally transduced with an antibody/Fc-γ chain chimeric receptor gene recognizing a human ovarian cancer antigen. Nat Med 1998;4:168–72.
42. Pinthus JH, Waks T, Kaufman-Francis K, et al. Immuno-gene therapy of established prostate tumors using chimeric receptor-redirected human lymphocytes. Cancer Res 2003;63:2470–6.
43. Haynes NM, Trapani JA, Teng MW, et al. Single-chain antigen recognition receptors that costimulate potent rejection of established experimental tumors. Blood 2002;100:3155–63.
44. Patel SD, Ge Y, Moskalenko M, McArthur JG. Anti-tumor CC49-ζ CD4 T cells possess both cytolytic and helper functions. J Immunother 2000;23: 661–8.
45. Riviere I, Sadelain M, Brentjens RJ. Novel strategies for cancer therapy: the potential of genetically modified T lymphocytes. Curr Hematol Rep 2004;3:290–7.
46. Ma Q, Safar M, Holmes E, Wang Y, Boynton AL, Junghans RP. Anti-prostate specific membrane antigen designer T cells for prostate cancer therapy. Prostate 2004;61:12–25.
47. Pinthus JH, Waks T, Malina V, et al. Adoptive immunotherapy of prostate cancer bone lesions using redirected effector lymphocytes. J Clin Invest 2004;114: 1774–81.
48. Bander NH, Trabulsi EJ, Kostakoglu L, et al. Targeting metastatic prostate cancer with radiolabeled monoclonal antibody J591 to the extracellular domain of prostate specific membrane antigen. J Urol 2003; 170:1717–21.
49. Trabulsi EJ, Yao D, Joyce MA, et al. Phase I radioimmunotherapy (RIT) trials of monoclonal antibody (MAB) J591 to the extracellular domain of prostate specific membrane antigen (PSMAEXT) radiolabeled with ^{90}Yttrium (^{90}Y) or ^{177}Lutetium. American Urological Association annual meeting; Chicago, IL. 2003.
50. O'Keefe DS, Bacich DJ, Heston WD. Comparative analysis of prostate-specific membrane antigen (PSMA) versus a prostate-specific membrane antigen-like gene. Prostate 2004;58:200–10.

Downloaded from cancerres.aacrjournals.org on September 13, 2017. © 2005 American Association for Cancer Research.

AACR American Association for Cancer Research

Cancer Research
The Journal of Cancer Research (1916–1930) | The American Journal of Cancer (1931–1940)

Targeted Elimination of Prostate Cancer by Genetically Directed Human T Lymphocytes

Terence P.F. Gade, Waleed Hassen, Elmer Santos, et al.

Cancer Res 2005;65:9080-9088.

Updated version	Access the most recent version of this article at: http://cancerres.aacrjournals.org/content/65/19/9080
Supplementary Material	Access the most recent supplemental material at: http://cancerres.aacrjournals.org/content/suppl/2005/11/11/65.19.9080.DC1

Cited articles	This article cites 46 articles, 17 of which you can access for free at: http://cancerres.aacrjournals.org/content/65/19/9080.full#ref-list-1
Citing articles	This article has been cited by 9 HighWire-hosted articles. Access the articles at: http://cancerres.aacrjournals.org/content/65/19/9080.full#related-urls

E-mail alerts	Sign up to receive free email-alerts related to this article or journal.
Reprints and Subscriptions	To order reprints of this article or to subscribe to the journal, contact the AACR Publications Department at pubs@aacr.org.
Permissions	To request permission to re-use all or part of this article, contact the AACR Publications Department at permissions@aacr.org.

Downloaded from cancerres.aacrjournals.org on September 13, 2017. © 2005 American Association for Cancer Research.